# The Constant Modulus Array for Cochannel Signal Copy and Direction Finding

John J. Shynk, *Senior Member, IEEE,* and Richard P. Gooch, *Member, IEEE*

*Abstract*—**The constant modulus (CM) array is a blind adaptive beamformer capable of recovering a narrowband signal among several cochannel sources without using a pilot or training signal. It is a conventional weight-and-sum adaptive beamformer whose weights are updated by the constant modulus algorithm. An adaptive signal canceller follows the beamformer to remove the captured signal from the array input and to provide an estimate of its direction vector. Based on a Wiener model, we investigate the steady-state properties of the CM array and the signal canceller. For mutually uncorrelated sources and noise, it is shown that the signal canceller exactly removes the source captured by the array. Thus, identical stages of the CM array and signal canceller may be used in a multistage system to recover several cochannel sources. Computer simulations are presented to verify the analytical results and to illustrate the transient behavior of the system.**

## I. Introduction

In CELLULAR radio systems, spectral crowding and cochannel interference are becoming increasingly important issues as the number of subscribers grows. Cochannel interference results from frequency reusage, whereby multiple cells operate on the same carrier frequency [1]. Depending on geographic considerations and environmental conditions, cochannel interference can be the dominant channel impairment. It would be desirable to incorporate "smart" directional antennas into the cellular system that are capable of reducing the effects of cochannel interference and in turn allow greater frequency reusage. These antennas should be capable of simultaneously estimating the angles of arrival (AOA's) of several cochannel sources, as well as demodulating the signals themselves (referred to as signal copy).

In recent years, there has been much interest in blind cochannel signal copy algorithms for antenna arrays. For example, a class of blind adaptive algorithms was developed in [2] that extracts and separates multiple signals-of-interest on the basis of their differing spectral self-coherence strengths. Spectral self-coherence refers to the property of a communication signal whereby it is correlated with a frequency-shifted version of itself. Another approach is the two-step procedure described in [3] and [4] that incorporates a high-resolution direction-finding algorithm followed by a maximum-likelihood scheme to estimate the sources. A signal subspace method, such as the MUSIC (multiple signal classification) algorithm [5], is employed to estimate the AOA's. More recently, a decision-feedback approach was presented in [6] for the demodulation of digital signals. Symbol decisions based on preliminary signal estimates are used to regenerate the signal waveforms from which improved estimates are derived.

The CM array is an adaptive beamformer designed to blindly recover a cochannel signal [7]. It has a conventional weight-and-sum beamformer configuration [8] and its weights are adapted by the constant modulus algorithm (CMA) [9]. The CM array has fast convergence properties and low computational complexity. Moreover, its signal copy performance is insensitive to array imperfections. The multistage CM array consists of a cascade of individual CM array stages [10]–[12]. An adaptive signal canceller is included in each stage to remove a captured source from the input before subsequent processing by the follow-on stages.

In this paper, we analyze the steady-state properties of the CM array and the signal canceller corresponding to one stage of a multistage system. A steady-state analysis of the other stages, which is an extension of the work presented here, is given in [13]. We examine the case of uncorrelated sources in additive white Gaussian noise; the behavior of the cascade system for correlated sources (e.g., due to multipath in an urban environment) is briefly discussed. The case of correlated sources is more fully investigated in [14]–[16], which also describe parallel implementations of the multistage CM array.

This paper is organized as follows. Section II defines the array and signal models. In Section III, we give details about the CM array/signal canceller and the corresponding adaptive algorithms. The steady-state properties of the system are derived in Section IV, and computer simulation examples are presented in Section V. Although this paper focuses on the steady-state properties of the CM array (i.e., for stationary sources), we also include simulations to illustrate the tracking behavior of the system when one of the sources experiences Rayleigh fading. Finally, conclusions of this work are outlined in Section VI.

## II. Array and Signal Models

A block diagram of the system is shown in Fig. 1. We assume that the antenna elements are uniformly spaced and omnidirectional such that we can write the array input signals

Manuscript received May 10, 1994; revised September 15, 1995. This work was supported by Applied Signal Technology, Inc., by the University of California MICRO Program, and by the National Science Foundation under Grant MIP 9308919. The associate editor coordinating the review of this paper and approving it for publication was Prof. Michael P. Clark.

J. J. Shynk is with the Department of Electrical and Computer Engineering, University of California, Santa Barbara, CA 93106 USA (e-mail: shynk@ece.ucsb.edu).

R. P. Gooch is with Applied Signal Technology, Inc., Sunnyvale, CA 94086 USA.

Publisher Item Identifier S 1053-587X(96)02393-6.

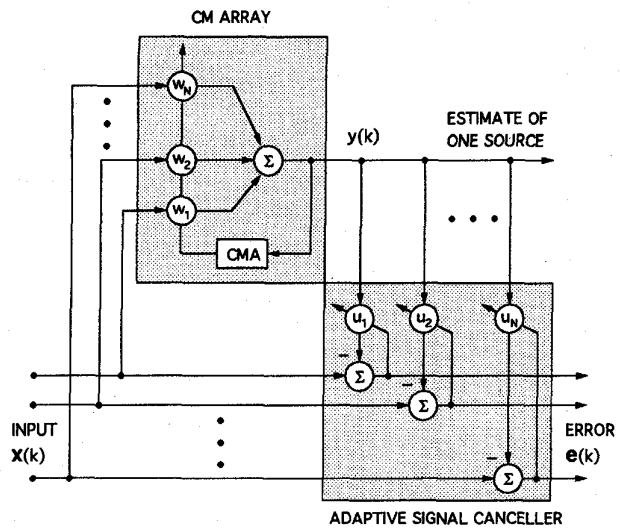


Fig. 1. Constant modulus array and adaptive signal canceller.

as

$$x_m(t) = \sum_{l=1}^{L} s_l(t)e^{-j(m-1)\phi_l} + n_m(t), \qquad m = 1, \cdots, N \tag{1}$$

where $\{s_l(t)\}$ are the $L$ (baseband) sources and $\{n_m(t)\}$ are additive white Gaussian noise processes. Because the sources are narrowband, $\phi_l = 2\pi(d/\lambda)\sin(\theta_l)$ where $d$ is the interelement spacing, $\lambda$ is the wavelength of the sources, and $\{\theta_l\}$ are their angles of arrival. By collecting the signals into vectors and assuming that the $\{x_m(t)\}$ are sampled, we can rewrite (1) as

$$\boldsymbol{x}(k) = \boldsymbol{A}\boldsymbol{s}(k) + \boldsymbol{n}(k) \tag{2}$$

where $\boldsymbol{x}(k) \triangleq [x_1(k), \cdots, x_N(k)]^T$, $\boldsymbol{s}(k) \triangleq [s_1(k), \cdots, s_L(k)]^T$, $\boldsymbol{n}(k) \triangleq [n_1(k), \cdots, n_N(k)]^T$, and

$$\boldsymbol{A} \triangleq \begin{bmatrix} 1 & \cdots & 1 \\ e^{-j\phi_1} & \cdots & e^{-j\phi_L} \\ \vdots & \vdots & \vdots \\ e^{-j(N-1)\phi_1} & \cdots & e^{-j(N-1)\phi_L} \end{bmatrix}. \tag{3}$$

The columns $\{\boldsymbol{a}_i\}$ of $\boldsymbol{A}$ are known as direction vectors because they indicate the response of the array to a narrowband signal emanating from a particular direction. Note that although one is often interested in a uniform linear array as specified by (3), the signal copy performance of the CM array is independent of the array configuration [7]. Our analysis applies to a more general matrix $\boldsymbol{A}$. We should also mention that $L \leq N$ for the CM array, unlike most direction-finding algorithms (e.g., the MUSIC algorithm) where we must have $L < N$.

The correlation matrix of the data, defined as $\boldsymbol{R}_x \triangleq E[\boldsymbol{x}(k)\boldsymbol{x}^H(k)]$, is given by

$$\boldsymbol{R}_x = \boldsymbol{A}\boldsymbol{R}_s\boldsymbol{A}^H + \boldsymbol{R}_n \tag{4}$$

where $\boldsymbol{R}_s \triangleq E[\boldsymbol{s}(k)\boldsymbol{s}^H(k)]$ and $\boldsymbol{R}_n \triangleq E[\boldsymbol{n}(k)\boldsymbol{n}^H(k)]$. We assume that $\boldsymbol{s}(k)$ and $\boldsymbol{n}(k)$ are mutually uncorrelated with zero mean. Thus, $\boldsymbol{R}_s$ and $\boldsymbol{R}_n$ can be represented by the diagonal matrices $\Sigma_s$ and $\Sigma_n$, respectively. Furthermore, we assume the sensor noise powers are identical so that $\Sigma_n = \sigma_n^2\boldsymbol{I}$ and (4) becomes

$$\boldsymbol{R}_x = \boldsymbol{A}\Sigma_s\boldsymbol{A}^H + \sigma_n^2\boldsymbol{I}. \tag{5}$$

The $i$th diagonal component of $\Sigma_s$ is $\sigma_{s_i}^2 = E[|s_i(k)|^2]$, corresponding to the power of the $i$th source. It is well known that the rank of $\boldsymbol{A}\Sigma_s\boldsymbol{A}^H$ is $L$ (the number of sources with different AOA's) so that $N - L$ eigenvalues of $\boldsymbol{R}_x$ are equal to $\sigma_n^2$.

## III. CM Array and Adaptive Signal Canceller

The CM array estimates one component, $s_i(k)$, of $\boldsymbol{s}(k)$ from $\boldsymbol{x}(k)$ in an on-line adaptive manner without directly estimating $\boldsymbol{R}_x$. It also provides an estimate of the source direction vector $\boldsymbol{a}_i$ and, thus, the angle of arrival $\theta_i$. Observe in Fig. 1 that the input vector $\boldsymbol{x}(k)$ is processed by a weight-and sum beamformer, yielding the output

$$y(k) = \boldsymbol{w}^H(k)\boldsymbol{x}(k) \tag{6}$$

where $\boldsymbol{w}(k) \triangleq [w_1(k), \cdots, w_N(k)]^T$ are the adaptive weights adjusted by the constant modulus algorithm

$$\boldsymbol{w}(k+1) = \boldsymbol{w}(k) + 2\mu_{\text{cma}}\boldsymbol{x}(k)\epsilon_c^*(k) \tag{7}$$

with

$$\epsilon_c(k) = y(k)/|y(k)| - y(k). \tag{8}$$

The step size $\mu_{\text{cma}} > 0$ controls the convergence rate of (7), and the superscript $^*$ denotes complex conjugate. This update is identical to that of the complex least-mean-square (LMS) algorithm [8], except that the desired signal is replaced by $y(k)/|y(k)|$.

It has been shown for constant modulus signals that the capture behavior of the CM array depends on the initial weight vector $\boldsymbol{w}(0)$ and the relative signal powers at the array output. Specifically, for $L = N = 2$ sources (and a different version of CMA), it was demonstrated that the CM array will lock onto the source with the greatest power at the output of the array while nulling the other source [7]. It has been shown that the CM array will also capture nonconstant modulus sources provided the source kurtosis is $<2$ [17]. Since the array output primarily contains the captured source, a signal canceller may be used to remove $s_i(k)$ from $\boldsymbol{x}(k)$, generating a modified input vector that can be processed by a follow-on CM array stage in a multistage system [10], [13].

Observe in the figure that the signal canceller processes the array output via $\boldsymbol{u}(k) \triangleq [u_1(k), \cdots, u_N(k)]^T$ and then subtracts the result from the array input to yield an error vector

$$\boldsymbol{e}(k) = \boldsymbol{x}(k) - \boldsymbol{u}(k)y(k). \tag{9}$$

The canceller weights may be updated by a gradient-descent algorithm using

$$\boldsymbol{u}(k+1) = \boldsymbol{u}(k) + 2\mu_{\text{lms}}y^*(k)\boldsymbol{e}(k). \tag{10}$$

This recursion implements a set of $N$ independent single-weight LMS algorithm updates. It is straightforward to show

that for convergence in the mean, the step size is bounded by $0 < \mu_{\text{lms}} < 1/\sigma_y^2$ where $\sigma_y^2 = E[|y(k)|^2]$ is the variance of the CM array output (this variance is actually time-varying because the CM array weights are continually updated by (7)). Thus, the convergence properties of the canceller weights depend on those of the CM array, whereas the CM array weights are independent of the adaptive canceller. All canceller weights converge with the same time constant (because of the single input $y(k)$) given approximately by $\tau \approx 1/(2\mu_{\text{lms}}\sigma_y^2)$.

Substituting (6) into (9) yields a compact expression for the error vector

$$\boldsymbol{e}(k) = \boldsymbol{T}(k)\boldsymbol{x}(k) \tag{11}$$

where we have defined the signal transfer matrix

$$\boldsymbol{T}(k) \triangleq \boldsymbol{I} - \boldsymbol{u}(k)\boldsymbol{w}^H(k). \tag{12}$$

In a cascade multistage implementation, (11) corresponds to the input of the second stage. Thus, we are interested in the properties of $\boldsymbol{T}(k)$ at convergence, i.e., when the CM array has captured a cochannel source.

## IV. Steady-State Properties

### A. CM Array Wiener Weights

Assuming that the array captures the $i$th source, near convergence we may model the estimation error $\epsilon_c(k)$ as $\epsilon_i(k) = s_i(k) - y(k)$ [12]. At convergence, this error is orthogonal to the data, i.e., $E[\boldsymbol{x}(k)\epsilon_i^*(k)] = \boldsymbol{0}$, such that

$$E[\boldsymbol{x}(k)\boldsymbol{x}^H(k)]\boldsymbol{w}_o = E[\boldsymbol{x}(k)s_i^*(k)]. \tag{13}$$

This result follows by minimizing, with respect to $\boldsymbol{w}_o$, the following (conditional) mean-square error (MSE):

$$\xi = E[|s_i(k) - y(k)|^2|\boldsymbol{w}_o]. \tag{14}$$

The converged weight vector is given by $\boldsymbol{w}_o = \boldsymbol{R}_x^{-1}\boldsymbol{p}_i$ where $\boldsymbol{R}_x$ is the data autocorrelation matrix in (5) and $\boldsymbol{p}_i = E[\boldsymbol{x}(k)s_i^*(k)]$ is the cross-correlation vector associated with the captured source. Substituting $\boldsymbol{x}(k)$ from (2) yields $\boldsymbol{p}_i = \sigma_{s_i}^2\boldsymbol{a}_i$ and, thus, the following convergence point:

$$\boldsymbol{w}_o = \sigma_{s_i}^2\boldsymbol{R}_x^{-1}\boldsymbol{a}_i \tag{15}$$

where $\boldsymbol{a}_i$ is the $i$th column of the array matrix $\boldsymbol{A}$. The CM array output power $\sigma_{y_o}^2 = \boldsymbol{w}_o^H\boldsymbol{R}_x\boldsymbol{w}_o$ is given by

$$\sigma_{y_o}^2 = \sigma_{s_i}^4\boldsymbol{a}_i^H\boldsymbol{R}_x^{-1}\boldsymbol{a}_i = \boldsymbol{p}_i^H\boldsymbol{R}_x^{-1}\boldsymbol{p}_i \tag{16}$$

where (15) has been substituted for $\boldsymbol{w}_o$. Observe that since the minimum MSE is

$$\xi_{\min} = \sigma_{s_i}^2 - \boldsymbol{p}_i^H\boldsymbol{R}_x^{-1}\boldsymbol{p}_i \geq 0 \tag{17}$$

we must have $\boldsymbol{p}_i^H\boldsymbol{R}_x^{-1}\boldsymbol{p}_i \leq \sigma_{s_i}^2$ and, thus, from (16)

$$\sigma_{y_o}^2 \leq \sigma_{s_i}^2. \tag{18}$$

The output power of the CM array at convergence is bounded above by the power of the captured source.

The convergence point in (15) is based on the assumption that the CM array captures $s_i(k)$. Alternatively, we may view it as the desired result (and the optimal solution) if, in fact, we did have access to the $i$th source. Because CMA is a blind algorithm, the Wiener solution in (15) approximates the actual convergence point. However, simulations indicate that the above result is accurate for moderate-to-high signal-to-noise ratio (SNR) conditions (see the examples in Section V). We should also point out that since the CMA cost function is insensitive to phase variations, the algorithm in (7) will converge approximately to a scaled version of (15). This is discussed further in Section V in connection with the performance measures employed in the computer simulations.

### B. Signal Canceller Wiener Weights

To investigate the steady-state properties of the signal canceller, assume the CMA weights are fixed (converged) at $\boldsymbol{w}_o$. Taking the expected value of (10) and setting $E[\boldsymbol{u}(k+1)] = E[\boldsymbol{u}(k)] = \boldsymbol{u}_o$ yields

$$E[y^*(k)\boldsymbol{x}(k)] = E[|y(k)|^2]\boldsymbol{u}_o. \tag{19}$$

Solving for $\boldsymbol{u}_o$, we obtain the following convergence point for the canceller LMS algorithm:

$$\boldsymbol{u}_o = \boldsymbol{R}_x\boldsymbol{w}_o/\sigma_{y_o}^2. \tag{20}$$

In the terminology used to describe the Wiener solution in (15), $1/\sigma_{y_o}^2$ corresponds to the inverse autocorrelation (which is a scalar here because of the single input), and $\boldsymbol{R}_x\boldsymbol{w}_o$ is the cross-correlation vector (analogous to $\boldsymbol{p}_i$ above).

Substituting the optimal CM array weights from (15) into (20) yields

$$\boldsymbol{u}_o = (\sigma_{s_i}^2/\sigma_{y_o}^2)\boldsymbol{a}_i. \tag{21}$$

Note that the correlation matrix $\boldsymbol{R}_x$ in (20) has been cancelled by its inverse in (15). Thus, we see that the converged canceller weight vector is proportional to the $i$th direction vector of the array matrix $\boldsymbol{A}$. A calibrated look-up table could be used to obtain the corresponding AOA. Note that the direction-vector estimate is not biased by the additive noise (assuming the SNR is sufficiently large so that the model is valid and $s_i(k)$ is captured) since a scalar gain change in (21) modifies all components of the direction vector equally (the noise power $\sigma_n^2$ influences $\boldsymbol{u}_o$ via $\sigma_{y_o}^2$).

### C. Canceller Error Vector

Next, we investigate the effect of the previous results on the canceller error $\boldsymbol{e}(k)$. At convergence, the error vector is

$$\begin{aligned}\boldsymbol{e}_o(k) &= \boldsymbol{T}_o\boldsymbol{x}(k) = \boldsymbol{T}_o\boldsymbol{A}\boldsymbol{s}(k) + \boldsymbol{T}_o\boldsymbol{n}(k) \\ &= \boldsymbol{A}_e\boldsymbol{s}(k) + \boldsymbol{T}_o\boldsymbol{n}(k)\end{aligned} \tag{22}$$

where the converged signal transfer matrix is given by $\boldsymbol{T}_o \triangleq \boldsymbol{I} - \boldsymbol{u}_o\boldsymbol{w}_o^H$ and we have defined the effective array matrix $\boldsymbol{A}_e \triangleq \boldsymbol{T}_o\boldsymbol{A}$.

Consider the form of $\boldsymbol{A}_e$ and its influence on the source vector $\boldsymbol{s}(k)$. Substituting (15) and (21) yields

$$\begin{aligned}\boldsymbol{A}_e &= [\boldsymbol{I} - \boldsymbol{a}_i\boldsymbol{a}_i^H\boldsymbol{R}_x^{-1}/(\boldsymbol{a}_i^H\boldsymbol{R}_x^{-1}\boldsymbol{a}_i)]\boldsymbol{A} \\ &= \boldsymbol{A} - (1/\alpha_{i,i})\boldsymbol{a}_i\boldsymbol{a}_i^H\boldsymbol{R}_x^{-1}\boldsymbol{A} \end{aligned} \tag{23}$$

where for convenience we have defined $\alpha_{i,j} \triangleq \boldsymbol{a}_i^H\boldsymbol{R}_x^{-1}\boldsymbol{a}_j$. Observe that $\boldsymbol{A}$ may be partitioned into its columns so that

$$\begin{aligned}\boldsymbol{A}_e &= \boldsymbol{A} - (1/\alpha_{i,i})\boldsymbol{a}_i[\alpha_{i,1}, \cdots, \alpha_{i,i}, \cdots, \alpha_{i,L}] \\ &= \boldsymbol{A} - \boldsymbol{a}_i[\beta_{i,1}, \cdots, 1, \cdots, \beta_{i,L}] \end{aligned} \tag{24}$$

where $\beta_{i,j} \triangleq \alpha_{i,j}/\alpha_{i,i}$. Thus, the $i$th column of $\boldsymbol{A}_e$ is zero and all other columns are shifted, as in the following:

$$\boldsymbol{A}_e = [\boldsymbol{a}_1 - \beta_{i,1}\boldsymbol{a}_i, \cdots, \boldsymbol{0}, \cdots, \boldsymbol{a}_L - \beta_{i,L}\boldsymbol{a}_i]. \tag{25}$$

As a result, the $i$th source is completely cancelled (regardless of the additive noise power $\sigma_n^2$). The effective direction vectors are the original direction vectors minus scaled versions of $\boldsymbol{a}_i$. However, it is shown in the next section that $\beta_{i,j} \approx 0$ when the sources are not closely spaced (i.e., when the angles of arrival $\{\theta_i\}$ are not very similar).

### D. Shift Factors $\{\beta_{i,j}\}$

We refer to the $\{\beta_{i,j}\}$ as "shift factors." It is shown in Appendix A that

$$\beta_{i,j} = \frac{g_{i,j} - \boldsymbol{g}_i^H(\Sigma_{\text{snr}}^{-1} + \boldsymbol{G})^{-1}\boldsymbol{g}_j}{N - \boldsymbol{g}_i^H(\Sigma_{\text{snr}}^{-1} + \boldsymbol{G})^{-1}\boldsymbol{g}_i} \tag{26}$$

where $\boldsymbol{G} \triangleq \boldsymbol{A}^H\boldsymbol{A}$ is an $L \times L$ matrix with columns $\{\boldsymbol{g}_i\}$ and components $g_{i,j} \triangleq \boldsymbol{a}_i^H\boldsymbol{a}_j$. The diagonal matrix $\Sigma_{\text{snr}} \triangleq (1/\sigma_n^2)\Sigma_s$ has components $\{\sigma_{s_i}^2/\sigma_n^2\}$, which correspond to the source SNR's. Thus the shift factors $\{\beta_{i,j}\}$ are influenced directly by the AOA's of the various sources and, to a lesser degree, by their SNR's. This is easily seen from the closed-form expression below for the case of two sources (obtained by evaluating (26) for $L = 2$)

$$\beta_{1,2} = \frac{f(\phi_1, \phi_2)}{1 + N(1 - |f(\phi_1, \phi_2)|^2)(\sigma_{s_2}^2/\sigma_n^2)} \tag{27}$$

where

$$f(\phi_1, \phi_2) \triangleq \frac{1}{N}\frac{\sin[N(\phi_1 - \phi_2)/2]}{\sin[(\phi_1 - \phi_2)/2]}e^{j(N-1)(\phi_1 - \phi_2)/2}. \tag{28}$$

Fig. 2 shows an example of $|\beta_{1,2}|^2$ (log scale) versus $\theta_1$ for the case of $L = 2$ sources, $N = 3$ elements, $d = \lambda/2$, and an SNR of 20 dB (i.e., $\sigma_{s_1}^2 = \sigma_{s_2}^2 = 1$ and $\sigma_n^2 = 0.01$). The angles are measured normal to the linear array, and the direction of the second source is fixed at $\theta_2 = 45°$. Observe that the shift factor becomes significant only when the sources are closely spaced; otherwise, it is essentially zero.

It can be shown [18] that

$$|\beta_{i,j}|^2 = \frac{B(\theta_j)}{B(\theta_i)} \tag{29}$$

where

$$B(\theta) \triangleq |\boldsymbol{w}^H\boldsymbol{a}(\theta)|^2 \tag{30}$$

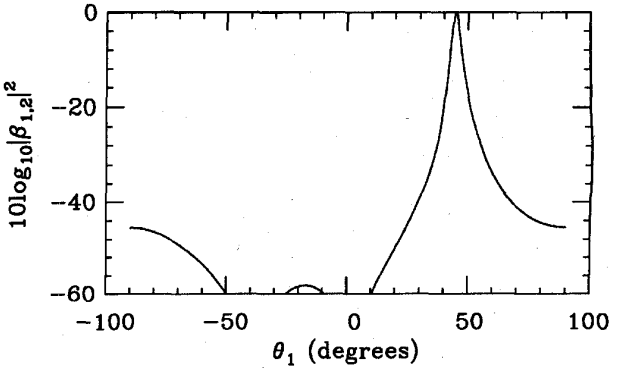


Fig. 2. Shift factor $|\beta_{1,2}|^2$ versus $\theta_1$. $N = 3, L = 2, \sigma_{s_1}^2 = \sigma_{s_2}^2 = 1$, $\sigma_n^2 = 0.01, \theta_2 = 45°$.

is the beampattern of the array weight vector. From this, we see that a shift factor is the ratio of the array gain at a null to that in the direction of the captured source. As a result, $\beta_{i,j}$ is also a measure of the resolution of the CM array. Fig. 3 shows two beampatterns associated with the $|\beta_{1,2}|^2$ plot in Fig. 2. The plots are normalized by the gain in the "look direction" $\theta_1$ (of the captured source); the dotted lines correspond to the array gains at the source AOA's. When the two sources are 45° apart, the nulled source is suppressed about 72 dB relative to the captured source. When the two sources are 5° apart, this difference is about 20 dB. These results are consistent with the $|\beta_{1,2}|^2$ plot in Fig. 2 and the relationship in (29).

### E. $\text{SINR}_{\text{out}}$ and $\text{SNR}_{\text{out}}$

The output signal-to-interference-plus-noise ratio $\text{SINR}_{\text{out}}$) is directly influenced by the $\{\beta_{i,j}\}$. It is shown in Appendix B that

$$\text{SINR}_{\text{out}} = \frac{\sigma_{s_i}^2}{\sum_{j \neq i}|\beta_{i,j}|^2\sigma_{s_j}^2 + (\boldsymbol{a}_i^H\boldsymbol{R}_x^{-2}\boldsymbol{a}_i/\alpha_{i,i}^2)\sigma_n^2}. \tag{31}$$

The corresponding expression for the input SINR is

$$\text{SINR}_{\text{in}} = \frac{\sigma_{s_i}^2}{\sum_{j \neq i}\sigma_{s_j}^2 + \sigma_n^2}. \tag{32}$$

Fig. 4 shows a plot of $\text{SINR}_{\text{out}}$ versus $\theta_1$ for the conditions used in Fig. 2. Comparing these two figures, we see that the $\text{SINR}_{\text{out}}$ decreases with increasing $|\beta_{1,2}|^2$, i.e., when the sources become closely spaced. By removing the cochannel interference term in (31), the output SNR is

$$\text{SNR}_{\text{out}} = (\sigma_{s_i}^2/\sigma_n^2)(\alpha_{i,i}^2/\boldsymbol{a}_i^H\boldsymbol{R}_x^{-2}\boldsymbol{a}_i) = \text{SNR}_{\text{in}}\frac{(\boldsymbol{a}_i^H\boldsymbol{R}_x^{-1}\boldsymbol{a}_i)^2}{\boldsymbol{a}_i^H\boldsymbol{R}_x^{-2}\boldsymbol{a}_i} \tag{33}$$

where $\text{SNR}_{\text{in}} \triangleq \sigma_{s_i}^2/\sigma_n^2$ is the input SNR of the $i$th source. An example of $\text{SNR}_{\text{out}}$ is also shown in Fig. 4. It is straightforward to show that $\text{SINR}_{\text{out}} \leq \text{SNR}_{\text{out}} \leq N \cdot \text{SNR}_{\text{in}}$ (see Appendix B).

From the previous results, we may conclude the following. (i) $\text{SINR}_{\text{out}} \approx \text{SNR}_{\text{out}}$ when the sources are not closely

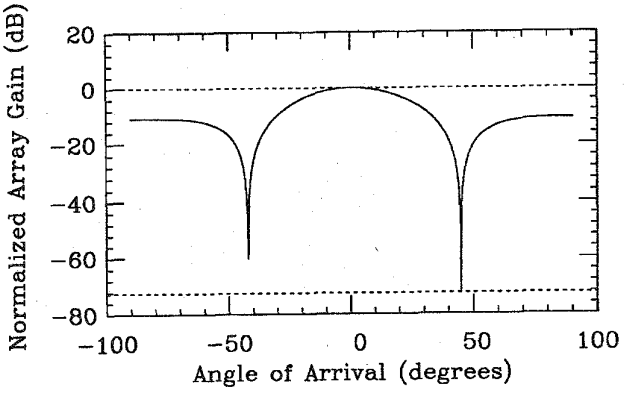


(a)

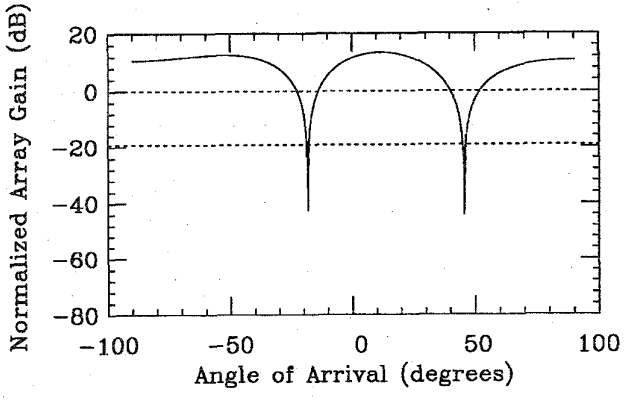


(b)

Fig. 3. Beampatterns based on the CM array Wiener weights. Same conditions as in Fig. 2. (a) $\theta_1 = 0°$. (b) $\theta_1 = 40°$.

spaced; i.e., the array at convergence nulls much of the interfering signal, and the noise dominates $\mathrm{SINR}_{\mathrm{out}}$. (ii) When $\theta_i \to \theta_j, |\beta_{i,j}|^2 \to 1$ and the signal canceller becomes less effective at removing the interfering source $s_j(k)$. The noise is enhanced and $s_j(k)$ begins to dominate $\mathrm{SINR}_{\mathrm{out}}$. (iii) When $\theta_i = \theta_j$, two columns of the array matrix $\boldsymbol{A}$ are identical and its rank becomes $L-1$. Although $\mathrm{SINR}_{\mathrm{out}} \approx \mathrm{SINR}_{\mathrm{in}}$, the noise is no longer enhanced ($\mathrm{SNR}_{\mathrm{out}}$ increases) because the two sources appear to be a single source.

### F. Properties of $\boldsymbol{T}_o$

The steady-state signal transfer matrix is

$$\boldsymbol{T}_o = \boldsymbol{I} - \frac{\boldsymbol{a}_i \boldsymbol{a}_i^H \boldsymbol{R}_x^{-1}}{\boldsymbol{a}_i^H \boldsymbol{R}_x^{-1} \boldsymbol{a}_i} = \boldsymbol{I} - \frac{\boldsymbol{a}_i \boldsymbol{b}_i^H}{\boldsymbol{b}_i^H \boldsymbol{a}_i} \tag{34}$$

where we have defined $\boldsymbol{b}_i \triangleq \boldsymbol{R}_x^{-1}\boldsymbol{a}_i$. From the form of this square matrix we observe the following properties. (i) $\boldsymbol{T}_o$ is idempotent ($\boldsymbol{T}_o^2 = \boldsymbol{T}_o$), corresponding to a (nonorthogonal) projection matrix (note that $\boldsymbol{T}_o^H \neq \boldsymbol{T}_o$). This property implies that if a follow-on stage were to have the same signal transfer matrix, the error vector would be unchanged. (The signal transfer matrices multiply from left to right along a cascade multistage implementation [13].) The first stage has successfully removed the captured source and no additional processing

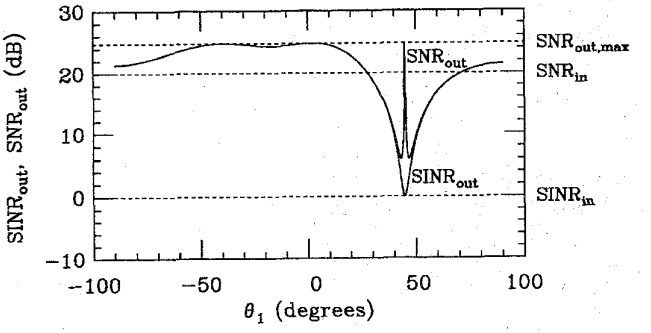


Fig. 4. $\mathrm{SINR}_{\mathrm{out}}$ and $\mathrm{SNR}_{\mathrm{out}}$ versus $\theta_1$. Same conditions as in Fig. 2.

is needed regarding that source. Of course, a follow-on stage would recover a different source and necessarily converge to a different signal transfer matrix. (ii) The eigenvalues of $\boldsymbol{T}_o$ are $(0, 1, \cdots, 1)$; thus, $\boldsymbol{T}_o$ is a singular matrix. Because the error correlation matrix $\boldsymbol{R}_e \triangleq E[\boldsymbol{e}(k)\boldsymbol{e}^H(k)]$ has the form $\boldsymbol{R}_e = \boldsymbol{T}_o \boldsymbol{R}_x \boldsymbol{T}_o^H$, this property demonstrates that $\boldsymbol{R}_e$ is a singular matrix (unlike $\boldsymbol{R}_x$). It is shown in [13] that this singularity does not adversely affect the steady-state properties of the other stages in a cascade multistage implementation. (iii) The eigenvector associated with the zero eigenvalue is $\boldsymbol{a}_i$; i.e., $\boldsymbol{a}_i$ lies in the null space of $\boldsymbol{T}_o$. From this, it immediately follows that the $i$th column of $\boldsymbol{A}_e = \boldsymbol{T}_o \boldsymbol{A}$ must be zero. This confirms the result in (25).

### G. Correlated Sources

Finally, we briefly consider the case of correlated sources and their effect on the canceller Wiener weight vector. Although the cascade CM array performs well in many signal environments (refer to the real-time implementation described in [19]), its performance will be diminished when the sources are highly correlated. This may occur, for example, in an urban area where there is significant multipath. A complete discussion of the results for correlated sources is beyond the scope of this paper; instead, we refer the reader to [14]–[16] for further details.

Consider the case of $L = 2$ sources with correlation coefficient $\rho_{12}$. Also, for convenience assume that $N = 2$ so that

$$\boldsymbol{R}_s = \begin{bmatrix} \sigma_{s_1}^2 & \sigma_{s_1}\sigma_{s_2}\rho_{12} \\ \sigma_{s_1}\sigma_{s_2}\rho_{12}^* & \sigma_{s_2}^2 \end{bmatrix}. \tag{35}$$

For this case, it is easy to show that the optimal CM array weights are

$$\boldsymbol{w}_o = \boldsymbol{R}_x^{-1} \boldsymbol{A} \boldsymbol{r}_{s,i} \tag{36}$$

where $\boldsymbol{r}_{s,i}$ is the $i$th column of $\boldsymbol{R}_s$ (corresponding to the $i$th captured source). The optimal canceller weights are still given by (20), which, after inserting (36), becomes

$$\boldsymbol{u}_o = \boldsymbol{A} \boldsymbol{r}_{s,i} / \sigma_{y_o}^2. \tag{37}$$

Note that $\sigma_{y_o}^2$ has the previous form $\sigma_{y_o}^2 = \boldsymbol{w}_o^H \boldsymbol{R}_x \boldsymbol{w}_o$, except that we substitute (36) for $\boldsymbol{w}_o$.

Assume the first source ($i = 1$) is captured so that

$$\boldsymbol{u}_o = (\sigma_{s_1}^2/\sigma_{y_o}^2)[\boldsymbol{a}_1 + (\sigma_{s_2}/\sigma_{s_1})\rho_{12}^*\boldsymbol{a}_2]. \quad (38)$$

Thus, we see that the optimal canceller weight vector is a linear combination of the two direction vectors; the influence of $\boldsymbol{a}_2$ is determined by the size of the correlation coefficient $\rho_{12}$ and the relative source powers. One can show that $s_1(k)$ is not completely cancelled by the transformation $\boldsymbol{T}_o$ [14], as it was for the uncorrelated case ($\rho_{12} = 0$). Both columns of the effective array matrix $\boldsymbol{A}_e$ are linear combinations of the original array response vectors $\boldsymbol{a}_1$ and $\boldsymbol{a}_2$.

## V. Computer Simulations

### A. Stationary Sources

The convergence behavior of the CM array and the signal canceller is illustrated by example computer simulations. There are $L = 3$ sources with the following angles of arrival: $\theta_1 = -10°, \theta_2 = 45°$, and $\theta_3 = 70°$, with equal variances $\sigma_{s_1}^2 = \sigma_{s_2}^2 = \sigma_{s_3}^2 = 1$. The number of CM array weights is $N = 3$, and they were initialized to $\boldsymbol{w}(0) = [1, 0, 0]^T$; the canceller weights were all initialized to zero $\boldsymbol{u}(0) = [0, 0, 0]^T$. The step sizes are $\mu_{\text{cma}} = 0.02$ and $\mu_{\text{lms}} = 0.01, d = \lambda/2$, and the noise power is $\sigma_n^2 = 0.01$. The random phases $\{\psi_i(k)\}$ of each source $s_i(k) = e^{j\psi_i(k)}$ were drawn independently from the uniform distribution $[-\pi, \pi]$.

Recall that the Wiener weight vector $\boldsymbol{w}_o$ minimizes the MSE in (14). Because CMA is insensitive to phase variations, it will in general converge approximately to a scaled version of $\boldsymbol{w}_o$. Thus, we utilize the following metric to quantify the performance of the CM array

$$\xi_{\text{cma},i}(k) = E[|s_i(k) - \gamma_i(k)y(k)|^2|\boldsymbol{w}(k)] \quad (39)$$

where $\gamma_i(k)$ is a complex scalar chosen to minimize (39). Note that this expression is conditioned on the CM array weight vector at time instant $k$; it can be plotted as a function of time for each value of the weight vector updated in (7). The scale factor $\gamma_i(k)$ may be viewed as an adaptive weight that aligns the phase components of $s_i(k)$ and $y(k)$. However, instead of adapting $\gamma_i(k)$ by an LMS-type algorithm, we may substitute the corresponding Wiener weight after each CMA update. It is straightforward to show that the $\gamma_i(k)$ minimizing (39) is given by

$$\gamma_i(k) = [\sigma_{s_i}^2/\sigma_y^2(k)]\boldsymbol{a}_i^H\boldsymbol{w}(k) \quad (40)$$

where $\sigma_y^2(k) = \boldsymbol{w}^H(k)\boldsymbol{R}_x\boldsymbol{w}(k)$ is the output variance (conditioned on $\boldsymbol{w}(k)$). Fig. 5(a) shows a trajectory of (39) for the captured source $s_1(k)$ (the expectation was approximated by averaging the squared error over 100 independent computer runs). Observe that convergence is quite fast; $s_1(k)$ is captured after about 400 samples. Furthermore, the minimum MSE (given by (17) and indicated by the dotted line) is nearly achieved. It is possible to lower the small amount of misadjustment shown by decreasing the step size. The corresponding converged weight vector is a scaled version of the Wiener solution $\boldsymbol{w}_o$ in (15), as follows:

$$\boldsymbol{w}_{o,\gamma_o} = (\gamma_o/|\gamma_o|^2)\boldsymbol{w}_o \quad (41)$$

where $\gamma_o$ is (40) at convergence.

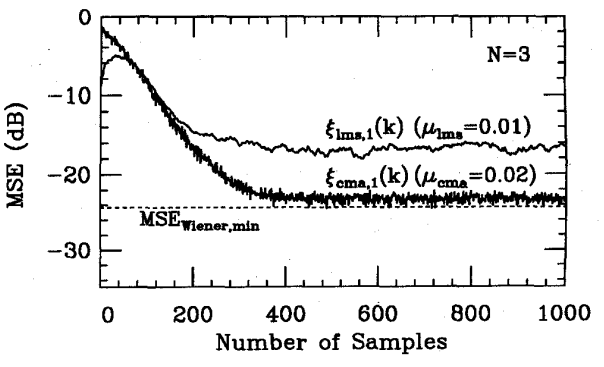


(a)

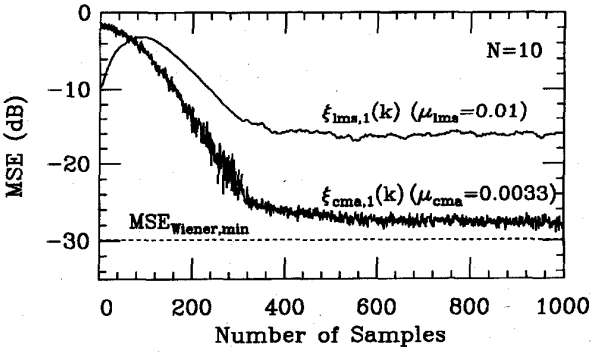


(b)

Fig. 5. MSE trajectories for the case of stationary sources. $L = 3, \sigma_{s_1}^2 = \sigma_{s_2}^2 = \sigma_{s_3}^2 = 1, \sigma_n^2 = 0.01$. (a) $N = 3$. (b) $N = 10, \eta = 0.5$.

The converged weight vector of the canceller is a scaled version of the Wiener solution $\boldsymbol{u}_o$ in (20), i.e.

$$\boldsymbol{u}_{o,\gamma_o} = \boldsymbol{R}_x\boldsymbol{w}_{o,\gamma_o}/\sigma_{y_o,\gamma_o}^2 \quad (42)$$

where $\sigma_{y_o,\gamma_o}^2$ is the output variance based on the scaled weight vector in (41). Substituting (41) yields

$$\boldsymbol{u}_{o,\gamma_o} = (\gamma_o/|\gamma_o|^2)\boldsymbol{R}_x\boldsymbol{w}_o/(\sigma_{y_o}^2/|\gamma_o|^2) = \gamma_o\boldsymbol{u}_o \quad (43)$$

where $\boldsymbol{u}_o$ is the Wiener solution in (20). Thus, the canceller weights are scaled by $\gamma_o$ at convergence. We can use this result to plot the trajectory of the canceller weight error, as follows:

$$\xi_{\text{lms},i}(k) = (1/N)E[||\boldsymbol{u}(k) - \gamma_i(k)\boldsymbol{u}_o||^2|\boldsymbol{w}(k), \boldsymbol{u}(k)]. \quad (44)$$

This expression is scaled by the number of canceller weights so that (39) and (44) have the same relative noise power. The trajectory of (44) is also shown in Fig. 5(a).

Next, simulation results for $N = 10$ (and $L = 3$) are shown in Fig. 5(b). Since the eigenvalue spread of $\boldsymbol{R}_x$ is quite large ($\lambda_{\max}/\lambda_{\min} \approx 1225$), we can expect that the overall convergence rate will be quite slow. This condition would occur even if we had direct access to the captured source $s_1(k)$ and used it in place of $y(k)/|y(k)|$ in (8). To improve the convergence rate of the algorithm, we may employ leakage in the update as follows:

$$\boldsymbol{w}(k+1) = (1 - 2\mu_{\text{cma}}\eta)\boldsymbol{w}(k) + 2\mu_{\text{cma}}\boldsymbol{x}(k)\epsilon_c^*(k) \quad (45)$$

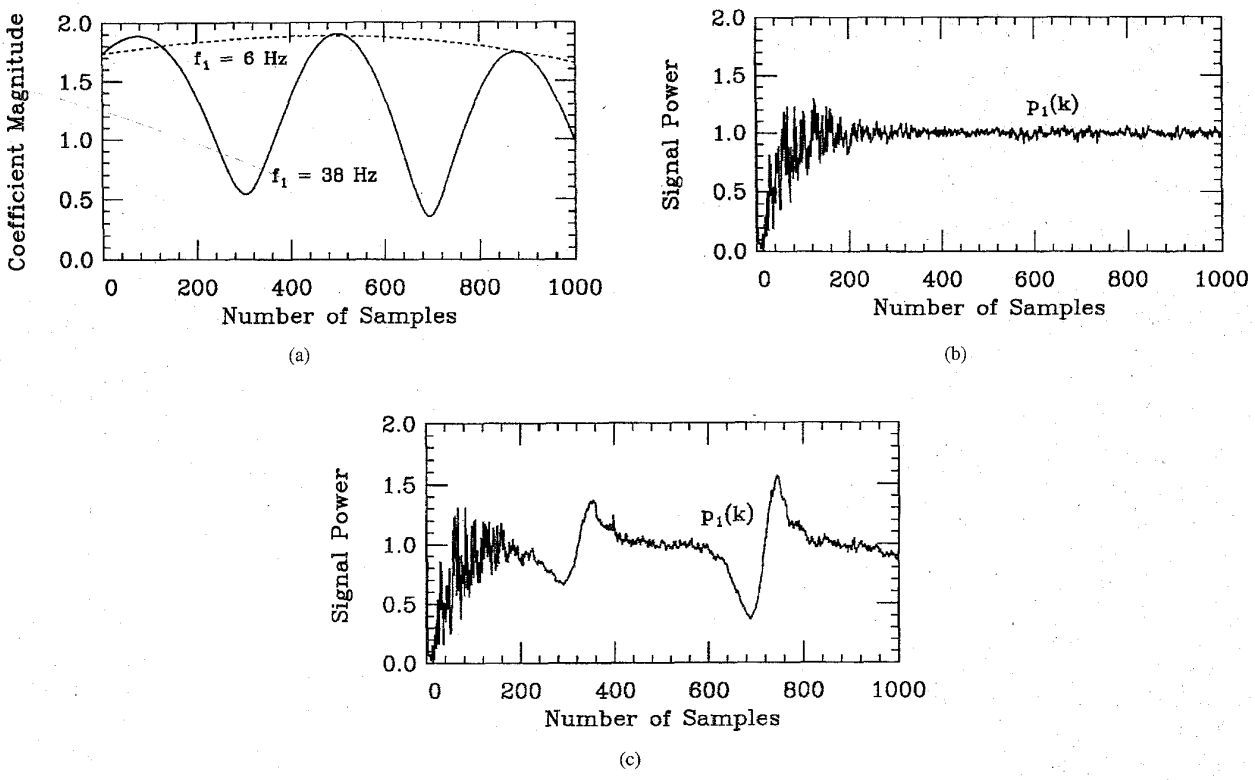


Fig. 6. Output signal power estimates for the case of a Rayleigh fading source. Same conditions as in Fig. 5(a). (a) Magnitude of the Rayleigh fading coefficient for two Doppler shifts; (b) trajectory for $f_1 = 6$ Hz; (c) trajectory for $f_1 = 38$ Hz.

where $0 \leq \eta < 1/\mu_{\text{cma}}$ is the leakage factor [20]. The CMA learning curve in the figure corresponds to $\eta = 0.5$ (leakage was not used in the canceller update). Observe that the convergence rate is similar to that for $N = 3$; furthermore, the algorithm nearly achieves the Wiener MSE (computed using (17)). The converged MSE of the canceller is essentially unchanged, so that the captured source is still effectively removed from the array input.

### B. Rayleigh Fading

Finally, we examine the capture and tracking performance of the CM array for a Rayleigh fading channel with Doppler shift. Using the model in [21], the time-varying factors that multiply the sources $\{s_m(k)\}$ are given by

$$h_m(k) = \sum_{n=1}^{M} c_n^{(m)} e^{j(\Omega_m k \cos \alpha_n^{(m)} + \phi_n^{(m)})} \tag{46}$$

where $\Omega_m = 2\pi f_m / f_s$, $f_m$ is the Doppler shift of the $m$th source, $f_s$ is the symbol rate, $\alpha_n^{(m)} = 2\pi n/M + \theta_n^{(m)}$, $\theta_n^{(m)}$ is uniform on $[-\delta, \delta]$ for some small $\delta$, and $\phi_n^{(m)}$ is a random phase uniform on $[-\pi, \pi]$. In our computer simulations, we used $\delta = 0.005$, $c_n^{(m)} = 1/\sqrt{M}$ (so that the $\{h_m(k)\}$ have unit power), $M = 14$ (so as to closely approximate a Rayleigh fading channel [21]), and $f_s = 24\,300$ baud (from the IS-54 standard [22]).

Using the above model, we show simulations when one of the sources has a Doppler shift and the other two sources are stationary. The trajectory (dashed line) in Fig. 6(a) is the coefficient magnitude of the fading source for a Doppler shift of 6 Hz (corresponding to a vehicle travelling 4.8 mph with a transmitting frequency of 850 MHz), assuming the data is transmitted at 24 300 baud. The Doppler shift $f_m$ and car velocity $v_m$ are related approximately as follows [23]: $f_m = (v_m/c) f_c$ Hz where $c$ is the speed of light and $f_c = 850$ MHz. Instead of plotting the MSE as was done in our previous simulations, we plot an estimate of the source power at the output of the array. This trajectory is shown in Fig. 6(b). The power estimate of the $i$th source is computed as

$$p_i(k) = |\boldsymbol{w}^H(k) \boldsymbol{a}_i h_i(k) s_i(k)|^2. \tag{47}$$

Note that only one run is shown in the figure, i.e., we did not average over 100 independent runs as was done for the MSE trajectories. The source and system parameters are the same as those used in Fig. 5(a).

Note that for this relatively mild case, the CM array captures and tracks the time-varying source. Fig. 6(c) shows the trajectory for a Doppler shift of 38 Hz (corresponding to 30.2 mph at a transmitting frequency of 850 MHz); the coefficient magnitude is shown in Fig. 6(a) (solid line). Observe that the CM array once again captures the time-varying source. However, its MSE performance is somewhat diminished; this is seen by the fact that the trajectory of $p_1(k)$ follows the coefficient in Fig. 6(a), whereas it should be near unity (because of the constant modulus property). Note, however, that larger step-size values may be used to compensate for

rapid variations in the source power. The transient properties of the CM array are investigated further in [13] and [24].

## VI. Conclusion

We have analyzed the steady-state properties of the constant modulus (CM) array whose output is processed by an adaptive signal canceller. This configuration may be used in a multistage system for the separation of several cochannel signals. When the CM array converges to the optimal solution, capturing one of the sources, the canceller exactly removes this signal. The canceller weights correspond to a scaled version of the direction vector of the captured source, from which it is possible to estimate its angle of arrival. Although the columns of the effective array matrix may be shifted away from the original direction vectors, it was shown that this bias is negligible if the sources are not too closely spaced and the SNR is adequate for the CM array to copy a source. The steady-state properties of a multistage system based on the CM array are investigated in [13] and an extension of this analysis to the case of correlated sources is considered in [14]–[16]. A real-time implementation of the multistage CM array with $N = 4$ elements is described in [19].

## Appendix A
## Evaluation of $\beta_{i,j}$

Recall that $\beta_{i,j} \triangleq \alpha_{i,j}/\alpha_{i,i}$ where $\alpha_{i,j} \triangleq \boldsymbol{a}_i^H \boldsymbol{R}_x^{-1} \boldsymbol{a}_j$, $\{\boldsymbol{a}_i\}$ are the columns of $\boldsymbol{A}$, and $\boldsymbol{R}_x$ is the correlation matrix in (5). From the matrix inversion lemma [20]

$$\boldsymbol{R}_x^{-1} = (1/\sigma_n^2)[\boldsymbol{I} - \boldsymbol{A}(\Sigma_{\text{snr}}^{-1} + \boldsymbol{A}^H\boldsymbol{A})^{-1}\boldsymbol{A}^H] \tag{A.1}$$

where $\Sigma_{\text{snr}} = (1/\sigma_n^2)\Sigma_s$ is a diagonal matrix with components given by the SNR's of the $L$ sources. For convenience, define $g_{i,j} \triangleq \boldsymbol{a}_i^H \boldsymbol{a}_j$. Observe that we can write

$$\alpha_{i,j} = (1/\sigma_n^2)[g_{i,j} - \boldsymbol{a}_i^H \boldsymbol{A}(\Sigma_{\text{snr}}^{-1} + \boldsymbol{A}^H\boldsymbol{A})^{-1}\boldsymbol{A}^H\boldsymbol{a}_j]. \tag{A.2}$$

If we partition $\boldsymbol{A}$ into its columns (as we did to derive (25)), this expression becomes

$$\begin{aligned}\alpha_{i,j} &= (1/\sigma_n^2)[g_{i,j} - [g_{i,1}, \cdots, g_{i,L}] \\ &\quad \cdot (\Sigma_{\text{snr}}^{-1} + \boldsymbol{A}^H\boldsymbol{A})^{-1}[g_{1,j}, \cdots, g_{L,j}]^T] \\ &= (1/\sigma_n^2)[g_{i,j} - \boldsymbol{g}_i^H(\Sigma_{\text{snr}}^{-1} + \boldsymbol{G})^{-1}\boldsymbol{g}_j]\end{aligned} \tag{A.3}$$

where $\boldsymbol{g}_i$ is the $i$th column of $\boldsymbol{G} \triangleq \boldsymbol{A}^H\boldsymbol{A}$ with components $\{g_{i,j}\}$. Inserting this expression into the definition of $\beta_{i,j}$ and cancelling the noise variance $\sigma_n^2$ yields the final result as follows:

$$\beta_{i,j} = \frac{g_{i,j} - \boldsymbol{g}_i^H(\Sigma_{\text{snr}}^{-1} + \boldsymbol{G})^{-1}\boldsymbol{g}_j}{N - \boldsymbol{g}_i^H(\Sigma_{\text{snr}}^{-1} + \boldsymbol{G})^{-1}\boldsymbol{g}_i} \tag{A.4}$$

where we have substituted $g_{i,i} = N$, the number of antenna elements.

## Appendix B
## Evaluation of $\text{SINR}_{\text{out}}$ and $\text{SNR}_{\text{out}}$

The output of the CM array at convergence is given by $y_o(k) = \boldsymbol{w}_o^H \boldsymbol{x}(k)$, which, after substituting $\boldsymbol{w}_o$ from (15) and $\boldsymbol{x}(k)$ from (2) becomes

$$y_o(k) = \sigma_{s_i}^2 \boldsymbol{a}_i^H \boldsymbol{R}_x^{-1}\boldsymbol{A}\boldsymbol{s}(k) + \sigma_{s_i}^2 \boldsymbol{a}_i^H \boldsymbol{R}_x^{-1}\boldsymbol{n}(k). \tag{B.1}$$

Partitioning $\boldsymbol{A}$ into its columns and substituting $\alpha_{i,j} \triangleq \boldsymbol{a}_i^H \boldsymbol{R}_x^{-1}\boldsymbol{a}_j$ yields

$$\begin{aligned}y_o(k) &= \sigma_{s_i}^2 \sum_{j=1}^{L} \alpha_{i,j} s_j(k) + \sigma_{s_i}^2 \boldsymbol{a}_i^H \boldsymbol{R}_x^{-1}\boldsymbol{n}(k) \\ &= \sigma_{s_i}^2 \alpha_{i,i} s_i(k) + \sigma_{s_i}^2 \sum_{j \neq i} \alpha_{i,j} s_j(k) + \sigma_{s_i}^2 \boldsymbol{a}_i^H \boldsymbol{R}_x^{-1}\boldsymbol{n}(k) \\ &\triangleq s_c(k) + c(k) + v(k)\end{aligned} \tag{B.2}$$

where $s_c(k)$ is the captured source (scaled), $c(k)$ represents the cochannel (interfering) signals, and $v(k)$ is a noise term, all at the output of the CM array.

The output SINR is defined as

$$\text{SINR}_{\text{out}} \triangleq \frac{E[|s_c(k)|^2]}{E[|c(k)|^2] + E[|v(k)|^2]} \tag{B.3}$$

where we have assumed that the sources and noise are mutually uncorrelated. Substituting the terms from (B.2) (after cancelling the common $\sigma_{s_i}^2$ term) yields

$$\text{SINR}_{\text{out}} = \frac{\sigma_{s_i}^2 \alpha_{i,i}^2}{\sum_{j \neq i} |\alpha_{i,j}|^2 \sigma_{s_j}^2 + \sigma_n^2 \boldsymbol{a}_i^H \boldsymbol{R}_x^{-2} \boldsymbol{a}_i}. \tag{B.4}$$

Dividing the numerator and denominator by $\alpha_{i,i}^2$ and substituting $\beta_{i,j} \triangleq \alpha_{i,j}/\alpha_{i,i}$ yields the following final result:

$$\text{SINR}_{\text{out}} = \frac{\sigma_{s_i}^2}{\sum_{j \neq i} |\beta_{i,j}|^2 \sigma_{s_j}^2 + (\sigma_n^2/\alpha_{i,i}^2)\boldsymbol{a}_i^H \boldsymbol{R}_x^{-2} \boldsymbol{a}_i}. \tag{B.5}$$

The output SNR is obtained from (B.5) by ignoring the cochannel interference term in the denominator, as follows:

$$\text{SNR}_{\text{out}} = (\sigma_{s_i}^2/\sigma_n^2)(\alpha_{i,i}^2/\boldsymbol{a}_i^H \boldsymbol{R}_x^{-2}\boldsymbol{a}_i) = \text{SNR}_{\text{in}} \frac{(\boldsymbol{a}_i^H \boldsymbol{R}_x^{-1}\boldsymbol{a}_i)^2}{\boldsymbol{a}_i^H \boldsymbol{R}_x^{-2}\boldsymbol{a}_i}. \tag{B.6}$$

The term weighting $\text{SNR}_{\text{in}} = \sigma_{s_i}^2/\sigma_n^2$ can be written as

$$(\boldsymbol{a}_i^H \boldsymbol{R}_x^{-1}\boldsymbol{a}_i)^2/(\boldsymbol{a}_i^H \boldsymbol{R}_x^{-2}\boldsymbol{a}_i) = (\boldsymbol{a}_i^H \boldsymbol{b}_i)^2/(\boldsymbol{b}_i^H \boldsymbol{b}_i) \tag{B.7}$$

where we have substituted $\boldsymbol{b}_i \triangleq \boldsymbol{R}_x^{-1}\boldsymbol{a}_i$. Because the components of $\boldsymbol{a}_i$ all have unit magnitude, it is clear that

$$(\boldsymbol{a}_i^H \boldsymbol{b}_i)^2 = \left(\sum_{k=1}^{N} e^{j(k-1)\phi_i} b_{i,k}\right)^2 \leq N \sum_{k=1}^{N} |b_{i,k}|^2 = N \boldsymbol{b}_i^H \boldsymbol{b}_i. \tag{B.8}$$

Thus, the expression in (B.7) is $\leq N$ so that $\text{SINR}_{\text{out}} \leq \text{SNR}_{\text{out}} \leq N \cdot \text{SNR}_{\text{in}}$.

## ACKNOWLEDGMENT

The authors would like to thank A. V. Keerthi and A. Mathur for generating the plots in Figs. 3, 5, and 6.

## REFERENCES

[1] W. C. Y. Lee, *Mobile Cellular Telecommunications Systems.* New York: McGraw-Hill, 1989.
[2] B. G. Agee *et al.*, "Spectral self-coherence restoral: A new approach to blind adaptive signal extraction using antenna arrays," *Proc. IEEE*, vol. 78, pp. 753–767, Apr. 1990.
[3] B. Ottersten, R. Roy, and T. Kailath, "Signal waveform estimation in sensor array processing," in *Proc. 23rd Asilomar Conf. Signals, Syst. Comput.*, Pacific Grove, CA, Nov. 1989, pp. 787–791.
[4] G. Xu *et al.*, "Maximum likelihood detection of co-channel communications signals via exploitation of spatial diversity," in *Proc. 26th Asilomar Conf. Signals, Syst., Comput.*, Pacific Grove, CA, Oct. 1992, pp. 1142–1146.
[5] R. O. Schmidt, "Multiple emitter location and signal parameter estimation," in *Proc. RADC Spectrum Estimation Workshop*, Griffiss Air Force Base, NY, 1979, pp. 243–258, 1979; repr. *IEEE Trans. Antennas Propagat.*, vol. AP-34, pp. 276–280, Mar. 1986.
[6] A. Swindlehurst *et al.*, "Analysis of a decision directed beamformer,"*IEEE Trans. Signal Processing*, vol. 43, pp. 2920–2927, Dec. 1995.
[7] R. P. Gooch and J. D. Lundell, "The CM array: An adaptive beamformer for constant modulus signals," in *Proc. IEEE Int. Conf. Acoust., Speech, Signal Processing*, Tokyo, Japan, Apr. 1986, pp. 2523–2526.
[8] B. Widrow and S. D. Stearns, *Adaptive Signal Processing.* Englewood Cliffs, NJ: Prentice-Hall, 1985.
[9] J. R. Treichler and B. G. Agee, "A new approach to multipath correction of constant modulus signals," *IEEE Trans. Acoust., Speech, Signal Processing*, vol. ASSP-31, pp. 459–472, Apr. 1983.
[10] B. J. Sublett *et al.*, "Separation and bearing estimation of co-channel signals," in *Proc. IEEE Military Commun. Conf.*, Boston, MA, Oct. 1989, pp. 629–634.
[11] R. P. Gooch *et al.*, "Adaptive beamformers in communications and direction finding systems," in *Proc. 24th Asilomar Conf. Signals, Syst., Comput.*, Pacific Grove, CA, Nov. 1990, pp. 11–15.
[12] J. J. Shynk and R. P. Gooch, "Convergence properties of the multistage CMA adaptive beamformer," in *Proc. 27th Asilomar Conf. Signals, Syst., Comput.*, Pacific Grove, CA, Nov. 1993, pp. 622–626.
[13] J. J. Shynk *et al.*,"Steady-state analysis of the multistage constant modulus array," *IEEE Trans. Signal Processing*, vol. 44, to be published.
[14] A. Mathur *et al.*, "Estimation of correlated cochannel signals using the constant modulus array," in *Proc. IEEE Int. Conf. Commun.*, Seattle, WA, June 1995, pp. 1525–1529.
[15] A. V. Keerthi *et al.*, "A blind adaptive antenna system for the estimation of mutually correlated cochannel sources," in *Proc. IEEE Military Commun. Conf.*, San Diego, CA, Nov. 1995, pp. 1051–1055.
[16] A. Mathur *et al.*, "Convergence properties of the multistage CM array for correlated sources," *IEEE Trans. Signal Processing*, to be published.
[17] J. D. Lundell and B. Widrow, "Application of the constant modulus adaptive beamformer to constant and nonconstant modulus signals," in *Proc. 21st Asilomar Conf. Signals, Syst., Comput.*, Pacific Grove, CA, Nov. 1987, pp. 432–436.
[18] A. V. Keerthi *et al.*, "Direction-finding performance of the multistage CM array," in *Proc. 28th Asilomar Conf. Signals, Syst., Comput.*, Pacific Grove, CA, Nov. 1994, pp. 847–852.
[19] W. Hosseini *et al.*, "A real-time implementation of the multistage CMA adaptive beamformer," in *Proc. 27th Asilomar Conf. Signals, Syst., Comput.*, Pacific Grove, CA, Nov. 1993, pp. 643–646.
[20] S. Haykin, *Adaptive Filter Theory,* 2nd ed. Englewood Cliffs, NJ: Prentice-Hall, 1991.
[21] W. C. Jakes, Jr., "Multipath interference," in *Microwave Mobile Communications* W. C. Jakes, Jr., Ed. New York: Wiley, 1974, pp. 67–68.
[22] EIA/TIA IS-54: Dual-Mode Mobile Station—Base Station Compatibility Standard, Electronic Industries Association, Oct. 1990.
[23] R. Gagliardi, *Introduction to Communications Engineering.* New York: Wiley-Interscience, 1978.
[24] A. Mathur *et al.*, "A modified CM array algorithm for fading channels," in *Proc. 29th Asilomar Conf. Signals, Syst., Comput.*, Pacific Grove, CA, Oct. 1995.

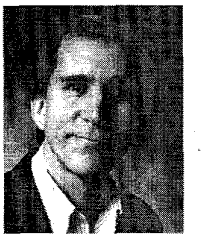

**John J. Shynk** (S'78–A'80–M'86–SM'91) received the B.S. degree in systems engineering from Boston University, Boston, MA, USA, in 1979 and the M.S. degree in electrical engineering and in statistics and the Ph.D. degree in electrical engineering from Stanford University, Stanford, CA, USA, in 1980, 1985, and 1987, respectively.

From 1979 to 1982, he was a Member of Technical Staff in the Data Communications Performance Group at AT&T Bell Laboratories, Holmdel, NJ, where he formulated performance models for voiceband data communications. He was a research assistant from 1982 to 1986 in the Department of Electrical Engineering at Stanford University, where he worked on frequency-domain implementations of adaptive IIR filter algorithms. From 1985 to 1986, he was also an instructor at Stanford University, teaching courses on digital signal processing and adaptive systems. Since 1987, he has been with the Department of Electrical and Computer Engineering at the University of California, Santa Barbara, CA, USA, where he is currently an associate professor. His research interests include adaptive signal processing, adaptive beamforming, wireless communications, direction-of-arrival estimation, and neural networks.

Dr. Shynk served as an associate editor for adaptive filtering of IEEE TRANSACTIONS ON SIGNAL PROCESSING and is currently an editor for adaptive signal processing of the INTERNATIONAL JOURNAL OF ADAPTIVE CONTROL AND SIGNAL PROCESSING and an associate editor for IEEE SIGNAL PROCESSING LETTERS. He is a member of Eta Kappa Nu, Tau Beta Pi, and Sigma Xi.

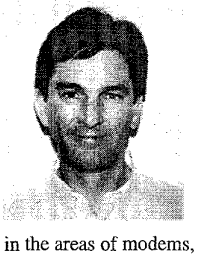

**Richard P. Gooch** (M'82) received the B.S. degree from the University of Illinois, Urbana-Champaign, USA, in 1978 and the Ph.D. degree from Stanford University, Stanford, CA, USA, in 1983, both in electrical engineering.

From 1983 to 1985, he was a research associate and lecturer at Stanford University. Since 1985, he has been with Applied Signal Technology, Sunnyvale, CA, USA where he is head of the Advanced Techniques Department. He is involved with the development of innovative algorithms and products in the areas of modems, wireless communications, and adaptive beamforming.